General atomic response to resonant, phase-fluctuating fields in the adiabatic limit

R. P. Frueholz and J. C. Camparo
Electronics Technology Center, The Aerospace Corporation, P.O. Box 92957, Los Angeles, California 90009
(Received 29 December 1994)

Though the interaction of a two-level atom with a field undergoing some arbitrary pattern of phase variation may be obtained by a numerical solution of the density-matrix equations, theory has proven to be problematic in providing a general, *intuitive* picture of the atom's response to a phase-varying field. The convolution picture of the fluctuating field-atom interaction, known to spectroscopists for decades, is only valid in the regime of weak fields. Here we discuss a complementary intuitive view that is valid in the regime of strong, resonant fields. Specifically, when an atom's response to a phase-varying field is considered in the instantaneous frame, the Bloch-vector trajectory always traces out a "figure-eight"–type pattern, reminiscent of a Lissajous figure. This observation is demonstrated for a number of fields whose phase-varying patterns span a broad range (i.e., sinusoidal, two-frequency quasiperiodic, chaotic, stochastic), and analysis of the Bloch-vector equations then reveals the complete generality of this response. The analysis also reveals that the temporal variation of the atomic population to phase fluctuations in the strong, resonant field regime is nearly proportional to a simple product of the field's phase and its first derivative.

PACS number(s): 42.50.Hz, 42.50.Ar, 32.80.Rm

I. INTRODUCTION

The response of quantum systems to resonant, phase-fluctuating electromagnetic fields is germane to several areas of current interest in atomic physics. In quantum optics, phase-modulated fields generate the Rabi-resonance phenomena [1,2], and stochastic phase fluctuations are known to alter some of the qualitative aspects of the field-atom interaction [3]. Further, atomic interactions with phase-fluctuating fields have been suggested as a means of producing supersonic light-induced gas streams [4], and increasing the gain coefficients associating with Lasing-Without inversion [5]. From an applied standpoint, an atom's response to a phase-modulated field is an important factor in a number of technologies, including, but not limited to, atomic frequency standards [6,7], optically pumped magnetometers [8], and laser frequency stabilization [9]. Our general interest in this topic stems from a desire to better understand the various factors that define and limit the performance of atomic frequency standards. In these devices a phase-modulated microwave field is often employed to generate the error signal used in locking a crystal oscillator's output frequency to an atomic hyperfine resonance, and future applications will require the locking to be stable at the level of a few parts in 10^{15}.

Though the interaction of a two-level atom with a field undergoing some arbitrary pattern of phase variation may be obtained by a numerical solution of the Bloch (i.e., density-matrix) equations [10], the theory has proven to be problematic in providing a general, *intuitive* picture of the atom's response to the phase-varying field. The convolution picture of the fluctuating field-atom interaction has, of course, been known to spectroscopists for decades, i.e., the field's phase variation is associated with some specific field spectrum, and a description of the field-atom interaction is obtained by convolving this field spectrum with the atomic response (i.e., line-shape) function. However, the convolution picture is only valid in the regime of weak fields, and there are a number of field-atom interaction topics where the assumption of weak fields is not justified. Consequently, the ultimate goal of our investigations, only partially achieved here, is the formulation of a general, intuitive picture of the fluctuating field-atom interaction that is valid in both weak and strong fields.

The starting point for the present studies is the analysis of Bloch-vector trajectories derived from a direct solution of the relevant differential equations. We find that under adiabatic conditions (adiabatic implying that the atomic Rabi frequency is much larger than the phase-modulation frequencies and atomic relaxation rate) there exist characteristics of an atom's response to a resonant field that are independent of any particular pattern of phase variation (stochastic or deterministic). As will be shown below, the physical explanation for these invariant characteristics derives from the Bloch equations when they are written for a coordinate frame that rotates at the field's instantaneous (fluctuating) frequency. Then, under adiabatic conditions, simple, general expressions relating the atomic response to the phase-modulation pattern may be derived.

II. DESCRIPTION OF SYSTEM UNDER ANALYSIS

The system under investigation is that of a two-level atom subjected to a resonant, phase-varying electromagnetic field. The Bloch equations for this system, under the assumption that the transverse and longitudinal relaxation rates are equal ($\gamma_1=\gamma_2=\gamma$), may be written as

$$\frac{dX}{dt}=-\gamma X-\Omega\cos[\theta(t)]Z\ , \tag{1a}$$

$$\frac{dY}{dt}=-\gamma Y-\Omega\sin[\theta(t)]Z\ , \tag{1b}$$

$$\frac{dZ}{dt}=-\gamma(Z-Z_{\rm NF})+\Omega\cos[\theta(t)]X+\Omega\sin[\theta(t)]Y\ . \tag{1c}$$

In these equations Ω is the Rabi frequency and X, Y, and Z are the coordinates of the Bloch vector in the rotating coordinate frame [11]. $Z_{\rm NF}$ is the Z value in the absence of any electromagnetic field, and $\theta(t)$ is the time-dependent phase of the field. If θ is constant, or varies extremely slowly, then under steady-state conditions the Bloch vector precesses about an effective field, whose orientation in the XY plane is given by θ. The inclusion of relaxation terms in the Bloch equations, beside mimicking realistic physical systems, ensures that after sufficient time any transient effects associated with the field's "turn on" will disappear.

In order to uncover general characteristics of the atom's response to a phase-fluctuating field, we have investigated four distinct phase-modulation patterns that span a broad range of characteristic types. The first two are relatively simple: (i) a pure sinusoidal phase modulation [Eq. (2a)], and (ii) a two-frequency quasiperiodic phase modulation with the two frequencies taken to be incommensurate [Eq. (2(b)]

$$\theta_S(t)=\pi\sin(\omega_1 t)\ , \tag{2a}$$

$$\theta_{\rm QP}(t)=\pi\sin(\omega_1 t)+\pi\sin(\omega_2 t)\ . \tag{2b}$$

In these equations ω_1 is set equal to 15 and ω_2 is set equal to ω_1 multiplied by five times the golden mean [golden mean $=(\sqrt{5}-1)/2$]. The third modulation pattern is associated with nonlinear chaos, and is produced by the solution of the nonlinear Duffing equation with its parameters chosen to yield chaotic variations [12]. The Duffing equation solved in this study takes the form

$$\frac{d^2P}{dt^2}+\Gamma A\frac{dP}{dt}-\tfrac{1}{2}A^2(1-P^2)P=FA\cos(A\omega t)\ , \tag{3}$$

with $\Gamma=0.09$, $F=0.16$, $\omega=0.833$, and $A=80.0$. (A is introduced as a simple time scale factor into the Duffing equation, in order to keep the various modulation patterns somewhat consistent.) The solution of the Duffing equation produces a phase variation $\theta_D(t)$ given by

$$\theta_D(t)=\pi P(t)/10\ . \tag{4}$$

The final phase-modulation pattern considered here is stochastic. It is produced by passing unit variance, Gaussian distributed white noise through a digital filter. The transfer function for the filter element, $H(f)$ is

$$H(f)=\frac{4\sigma_\theta}{\sqrt{3\alpha}}\frac{\alpha^3}{(2i\pi f+\alpha)^3}\ , \tag{5}$$

with f the Fourier frequency and $\alpha=25.0$. (This particular value of α was chosen in order to make the power spectrum of the random-phase variations reasonably similar to the power spectrum of the chaotic phase variations.) Transmission of white noise through a filter defined by Eq. (5) produces a white output for frequencies much less than $\alpha/2\pi$ and an output whose Fourier component amplitude falls as f^3 for frequencies much greater than $\alpha/2\pi$. σ_θ is the standard deviation of phase, and its value of 60° was selected in order to keep the amplitude of the phase variations consistent among the various phase modulation patterns. The procedure used here in the implementation of the digital filter is the same as that applied by Camparo and Lambropoulos [13] in their study of stochastic fields and multiphoton processes. Parameter values for the various modulation patterns were selected so that the principal frequency components of each occurred at similar frequencies. Figures 1(a) and 1(b) display the amplitude of the Fourier components for the chaotic and stochastic phase-variation processes, respectively.

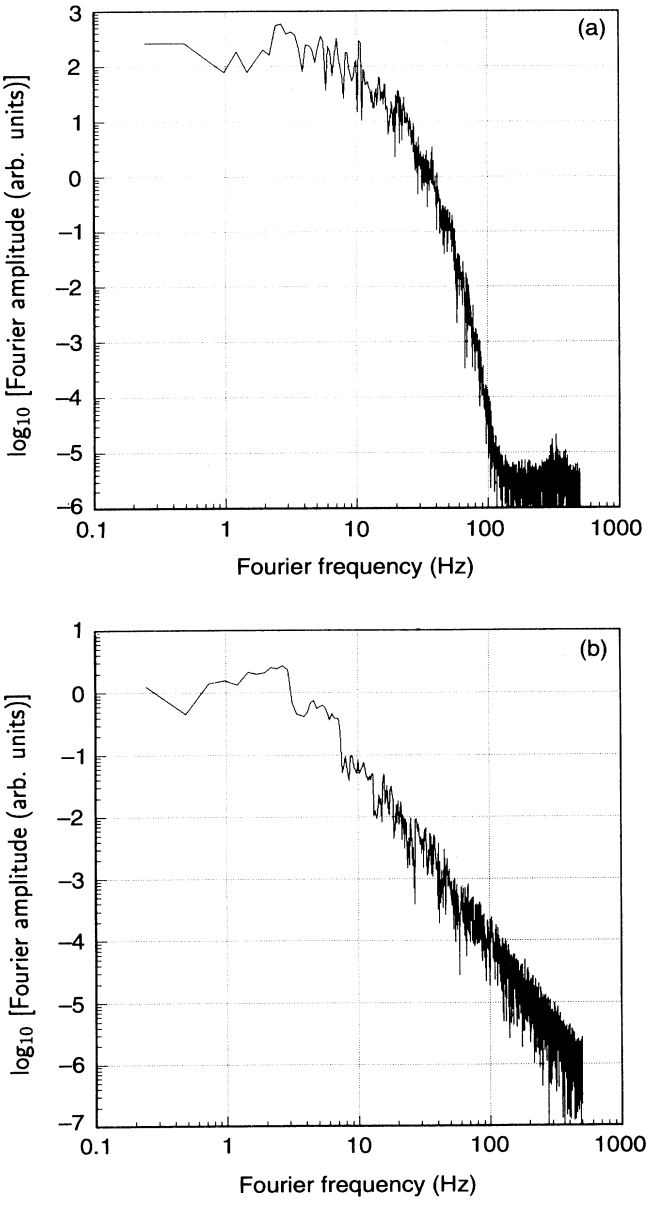

FIG. 1. Fourier transform of the phase variations generated by (a) chaotic, and (b) stochastic processes.

In the present study γ was taken as 0.5 and Z_{NF} was set equal to -1. The Bloch equations for each phase-modulation pattern were solved using a fourth-order Runge-Kutta algorithm with adaptive step size. For the chaotic phase variations, Eq. (3) was written as two first-order equations, combined with the three Bloch-vector equations. The resulting system of five equations was then solved simultaneously. In all cases, Runge-Kutta step size was controlled by requiring the relative error in the computation of any Bloch-vector component, as well as P and dP/dt for the case of the Duffing oscillator, to be less than 10^{-12} at each step. The initial conditions for the differential equations were $X(0)=0$, $Y(0)=0$, $Z(0)=1$, $P(0)=0$, and $dP(0)/dt=0$. To ensure that field turn-on transients had died away, the solutions were propagated to $t=40$ prior to analyzing the results.

III. RESULTS

We have found that the Bloch-vector trajectories resulting from our calculations are most informative when reviewed in the instantaneous frame described by Avan and Cohen-Tannoudji [14]. In this frame, the X^{inst} axis is taken along the direction of the effective field in the standard rotating frame (i.e., $\hat{X}^{inst}\cdot\hat{X}^{rot}=\cos[\theta(t)]$, where $\hat{X}^{rot}$ is a unit vector in the direction of the rotating frame X axis). For the case of a resonant field, the rotating frame and instantaneous frame are related by a simple time-dependent rotation in the XY plane. Previously, we found that quasiperiodic phase modulation produces a relatively simple atomic response when viewed in the instantaneous frame, as long as the Rabi frequency is sufficiently large to ensure adiabatic conditions [2]. This pattern and the phase modulation producing it are shown in Fig. 2. Extending our studies to the chaotic phase variations produced by the Duffing equation we observe the Bloch-space trajectories shown in Fig. 3. While differences in detail are observed, a general similarity is obvious: trajectories composed of two principal lobes are apparent in both cases. This is surprising given the differences in the modulation patterns, the amplitudes of phase variations [viz., compare Figs. 2(b) and 3(b)], and their concomitant differences in statistical and spectral properties.

Further numerical calculations have shown that this similarity of adiabatic atomic response remains valid over

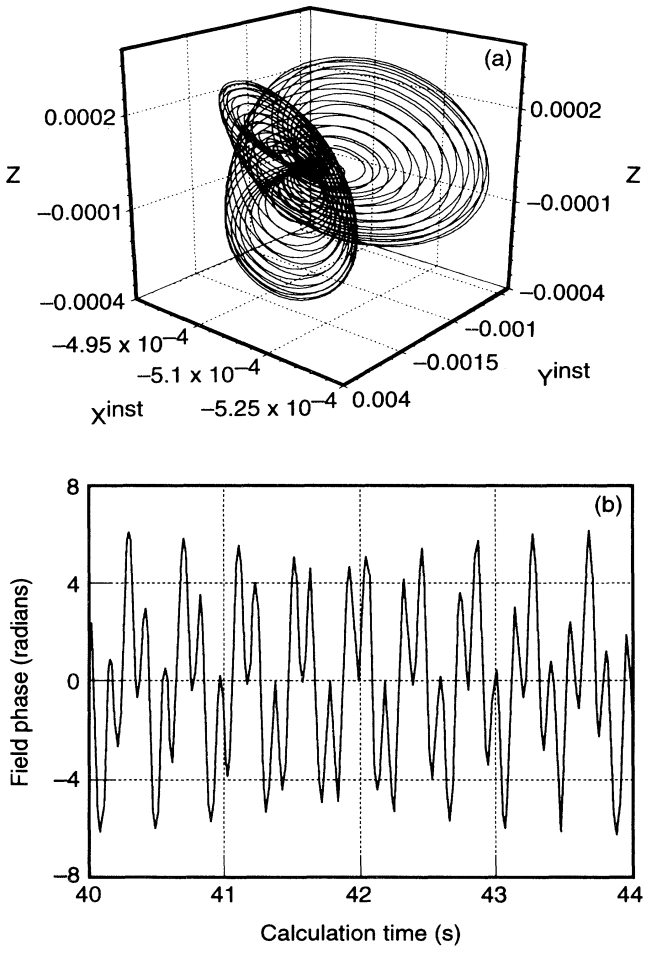

FIG. 2. (a) Bloch-space trajectory in the three-dimensional instantaneous frame resulting from quasiperiodic phase variation with $\Omega=1000$ (sufficient to ensure adiabatic atomic response). (b) Phase variation as a function of calculation time producing the Bloch-space trajectory of (a).

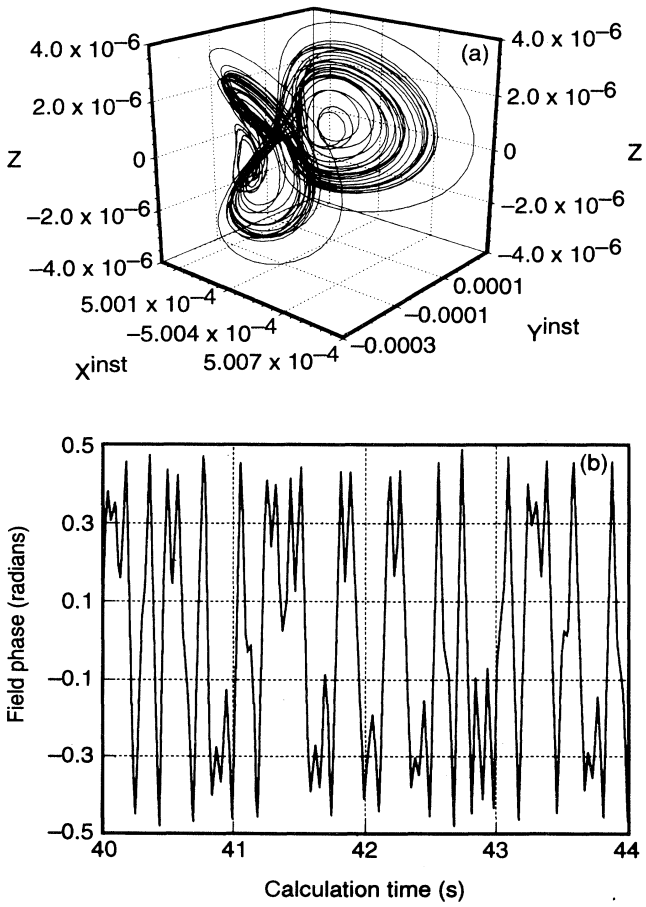

FIG. 3. Same as Fig. 2 except a chaotic phase variation is employed.

a wide range of phase-variation conditions. To highlight the similarities in the atom's response to different phase-modulation patterns, we project the three-dimensional trajectories onto the Y^{inst} and Z axes. In Fig. 4, the projected trajectories are shown for sinusoidal, quasiperiodic, chaotic, and stochastic patterns of phase variation. In all cases the two-lobed, "figure-eight-like" pattern is observed. For simple sinusoidal modulation the pattern is reminiscent of a Lissajous figure [15], in which the frequency of the vertical component is twice that of the horizontal component. It is this general figure-eight pattern, observed under resonant, adiabatic conditions, that we refer to as a general atomic response to phase-varying fields.

To understand the origin of this general atomic response, the Bloch equations in the rotating frame, Eqs. (1a)–(1c), may be transformed into the instantaneous frame yielding

$$\frac{dX^{\text{inst}}}{dt} = -\gamma X^{\text{inst}} + \frac{d\theta}{dt} Y^{\text{inst}} - \Omega Z \ , \tag{6a}$$

$$\frac{dY^{\text{inst}}}{dt} = -\gamma Y^{\text{inst}} - \frac{d\theta}{dt} X^{\text{inst}} \ , \tag{6b}$$

$$\frac{dZ}{dt} = -\gamma (Z - Z_{\text{NF}}) + \Omega X^{\text{inst}} \ . \tag{6c}$$

Note that the Z component is unaffected by the transformation, since the transformation is just a rotation in the XY plane. Further, it is to be noted that the transformed equations contain products of $d\theta(t)/dt$ and Bloch-vector components. Thus, the complete system of differential equations, the Bloch-vector equations plus the $\theta(t)$ and $d\theta(t)/dt$ equations, display a nonlinear character in the instantaneous frame. (This observation was also made a number of years ago by Allen and Eberly [10].) The existence of nonlinearities suggests that techniques often employed in the analysis of nonlinear differential equations might be fruitfully applied in the present analysis. Specifically, Eqs. (6) can be linearized in the vicinity of their equilibrium point, and the dynamics within this linear approximation investigated [16].

Taking X^{inst}, Y^{inst}, Z, θ, and $d\theta/dt$ as the components Q_j of a vector $\vec{\mathbf{Q}}$, and $\vec{\mathbf{F}}$ a function of $\vec{\mathbf{Q}}$, Eqs. (6) along with any functional information concerning θ and $d\theta/dt$ may be rewritten as

$$\frac{d\vec{\mathbf{Q}}}{dt} = \vec{\mathbf{F}}(\vec{\mathbf{Q}}) \ . \tag{7}$$

Linearization consists of expanding $\vec{\mathbf{F}}(\vec{\mathbf{Q}})$ in a Taylor series, and dropping terms of order $\vec{\mathbf{Q}}^2$ and higher. The resulting linear approximation is then given by

$$\vec{\mathbf{F}}(\vec{\mathbf{Q}}) \cong \overleftrightarrow{\mathbf{J}} \cdot \vec{\mathbf{Q}} \ , \tag{8}$$

with $\overleftrightarrow{\mathbf{J}}$ the Jacobian of $\vec{\mathbf{F}}$ defined by

$$J_{ij} = \left[\frac{\partial F_i}{\partial Q_j} \right]_{\vec{\mathbf{Q}} = \vec{\mathbf{Q}}_0} \ , \tag{9}$$

and $\vec{\mathbf{Q}}_0$ the equilibrium point. For the equilibrium values of θ and $d\theta/dt$ we consider their limit as the fluctuating

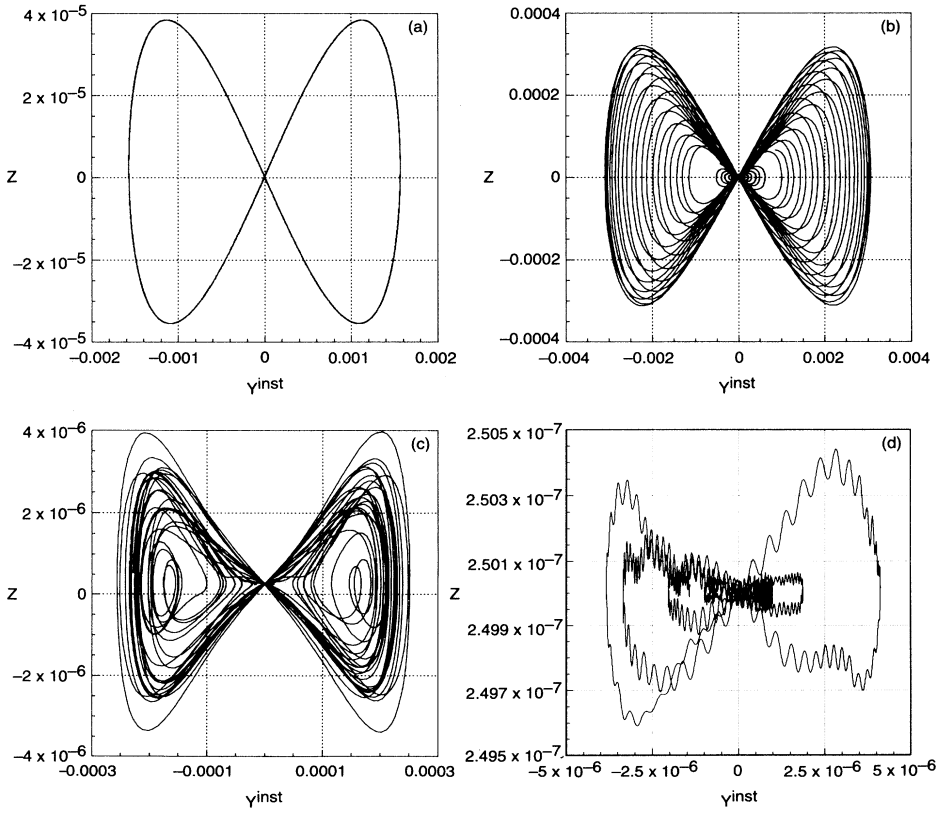

FIG. 4. Instantaneous frame Bloch-vector trajectories resulting from (a) sinusoidal, (b) quasiperiodic, (c) chaotic, and (d) stochastic phase variations projected on the Y^{inst} and Z axes.

amplitude of $\theta(t)$ becomes infinitesimally small, and without loss of generality these can be taken as zero. That $\theta_{eq}=0$ is simply a recognition of the fact that the phase variations of interest here fluctuate about a central value which may be taken as zero. Setting $(d\theta/dt)_{eq}=0$, however, has more physical justification, and is related to our focus on resonance conditions: any component of the phase variation that continuously increased or decreased would be considered a frequency offset, and its presence would not be consistent with resonance. For the equilibrium values of the Bloch-vector components, simple manipulations thus yield

$$X_{eq}^{inst}=-\frac{\gamma\Omega}{\gamma^2+\Omega^2}Z_{NF}\ , \tag{10a}$$

$$Y_{eq}^{inst}=0\ , \tag{10b}$$

$$Z_{eq}=\frac{\gamma^2}{\gamma^2+\Omega^2}Z_{NF}\ . \tag{10c}$$

The Jacobian may be evaluated using these values, and the resulting linearized Bloch equations then become

$$\frac{dX_L^{inst}}{dt}=-\gamma X_L^{inst}-\Omega Z_L\ , \tag{11a}$$

$$\frac{dY_L^{inst}}{dt}=-\gamma Y_L^{inst}+\left[\frac{\gamma\Omega Z_{NF}}{\gamma^2+\Omega^2}\right]\frac{d\theta}{dt}\ , \tag{11b}$$

$$\frac{dZ_L}{dt}=-\gamma Z_L+\Omega Y_L^{inst}\ . \tag{11c}$$

The principal advantage of this process is that the linearized form of Y^{inst}, Eq. (11b), is uncoupled from the X^{inst} and Z components, and may be related directly to the phase variations. If we assume that the phase varies rapidly compared with the relaxation rate, which is the condition of most interest, then formally integrating Eq. (11b) and then integrating by parts yields the approximate result,

$$Y_L^{inst}\cong\left[\frac{\gamma\Omega Z_{NF}}{\gamma^2+\Omega^2}\right]\theta\ . \tag{12}$$

To proceed, it is illuminating to now insert Eq. (12) into the full instantaneous frame Bloch equations for X^{inst} and Z, Eqs. (6a) and (6c). These equations form a set of two first-order, coupled differential equations in X^{inst} and Z, which may be written as a single second-order differential equation for Z:

$$\frac{d^2Z'}{dt^2}+2\gamma\frac{dZ'}{dt}+(\gamma^2+\Omega^2)Z'=\left[\frac{\gamma\Omega^2Z_{NF}}{\gamma^2+\Omega^2}\right]\theta\frac{d\theta}{dt}\ , \tag{13}$$

with $Z'=Z-Z_{eq}$. Equation (13) is simply that of a driven, damped harmonic oscillator. As a result of the relative size of the Rabi frequency with respect to the other constants in the problem (i.e., the adiabatic condition), it is apparent that the harmonic oscillator is far from resonance and that its "spring" is stiff. Consequently, we expect the Z' response to simply be proportional to the product of $\theta(t)$ and $d\theta(t)/dt$. The result of this adiabatic approximation is then

$$Z(t)=\left[\frac{\gamma\Omega^2Z_{NF}}{(\gamma^2+\Omega^2)^2}\right]\theta\frac{d\theta}{dt}+Z_{eq}\ . \tag{14}$$

The accuracy of these results may be tested by comparing the approximate values for $Y_L^{inst}(t)$ and $Z(t)$ with the exact results obtained by the numerical solution of the Bloch equations. In Fig. 5, for the case of chaotic phase variation and a Rabi frequency of 1000, the exact Y^{inst} and Z component values are compared with the approximate values produced by Eqs. (13) and (14). The agreement is very good, confirming the validity of the linearization approach used here. The approximate result for $Z(t)$ is particularly useful, as it is not restricted to either the instantaneous or rotating frames; the population variations it predicts will be those observed in the laboratory.

With the analytical results in hand, the origin of the general figure-eight Bloch-vector trajectory becomes ap-

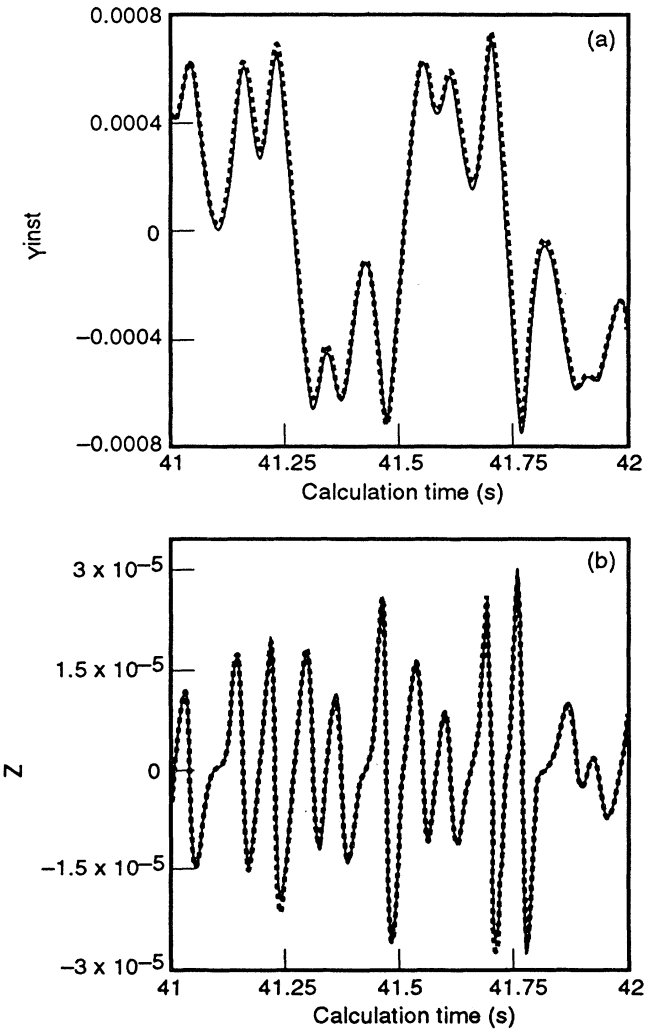

FIG. 5. Comparison of approximate values (dashed lines) of $Y^{inst}(t)$ [(a)] and $Z(t)$ [(b)] with the exact values (solid lines) resulting from numerical solution of the Bloch equations. In this example the Rabi frequency is taken to be 1000 and chaotic phase variations are employed.

parent. For any generally fluctuating pattern of phase variations, $\theta(t)$ and hence $Y^{\text{inst}}(t)$ will cross zero. Since $Z(t)$ is proportional to $Y^{\text{inst}}(t)$, as $Y^{\text{inst}}(t)$ approaches zero so too must $Z(t)$, producing the observed node in the ZY^{inst} plane. Within each of the lobes, the trajectories are defined by the specifics of the particular pattern of phase variation. The analytical results also give insight into the Lissajous pattern observed with single-sinusoidal phase modulation. In this case, $Y^{\text{inst}}(t)$ oscillates as $\sin(\omega_1 t)$, while $Z(t)$, proportional to the product $\cos(\omega_1 t)\sin(\omega_1 t)$, oscillates at twice the frequency of $Y^{\text{inst}}(t)$.

The final point to be addressed concerns the atomic response to the stochastic field shown in Fig. 4(d). Superimposed upon the general figure-eight trajectories are oscillations whose frequency matches that of the Rabi frequency. The presence of Rabi oscillations in the Bloch-vector trajectory indicates that some of the phase changes occur abruptly, so that the system is not adiabatic with respect to them. From an examination of the stochastic phase variation's Fourier spectrum, it may be inferred that the figure-eight pattern results from adiabaticity with respect to those Fourier components accounting for the largest spectral density (i.e., $f < 10$). The Rabi oscillations superimposed on the figure-eight pattern derive from nonadiabaticity associated with the high-frequency components of the Fourier spectrum. Note from Eq. (14) that the amplitude of the figure-eight pattern decreases as a function of Rabi frequency in the adiabatic regime. Consequently, for broadband noise an increase in Rabi frequency does not necessarily decrease the amplitude of the Rabi oscillations compared to the size of the figure-eight pattern. Interestingly, in calculations using stochastic phase-variation patterns where the high-frequency Fourier components fell more slowly (i.e., f^{-1} and f^{-2}), the adiabatic, figure-eight responses were completely overwhelmed by the nonadiabatic Rabi oscillations. These observations point out the significance of adiabaticity in the general atomic response to phase variations discussed here. Moreover, this highlighted role of adiabaticity clarifies why the chaotic phase variations produce such a well defined figure-eight pattern, even though they too have a broadband Fourier spectrum. Note that the Fourier spectrum for the chaotic phase variations falls off extremely rapidly at high Fourier frequency, so that it is possible to achieve a Rabi frequency where the spectral density at Fourier frequencies higher than the Rabi frequency is negligible. This issue of simultaneous adiabatic and nonadiabatic atomic responses for broadband phase variations will be explored in a future paper.

IV. SUMMARY AND CONCLUSIONS

In this paper we have investigated the response of a two-level atomic system to phase-varying fields under adiabatic conditions for a wide range of phase-variation patterns. Here, adiabatic means that the Rabi frequency is larger than the atomic relaxation rate and the phase-variation rate. Under adiabatic conditions we find that there is a general atomic response to the phase-varying field that is *independent* of the particular form of phase variation. This response is most apparent when Bloch-vector trajectories are observed in the instantaneous frame, and this frame is also found to be most appropriate for investigating the origins of the atom's general response. Analyses performed in this frame lead to a simple relationship between the two-level atom's population and the field's phase variations. We have also found that care must be exercised in defining what is meant by adiabatic when the pattern of phase variations displays a broadband Fourier spectrum. In this case, one might be tempted to term an atomic interaction adiabatic if a large enough Rabi frequency was achieved (e.g., so that a significant portion of the phase variation's spectral density occurred at Fourier frequencies smaller than this Rabi frequency). However, for broadband phase variations there will be some amount of spectral density at Fourier frequencies higher than this Rabi frequency, and these will give rise to a nonadiabatic response from the atom. The relative importance of these nonadiabatic contributions to the general atomic response discussed here likely depends on the specific shape of the Fourier spectrum at high Fourier frequencies.

ACKNOWLEDGMENT

The authors would like to thank Dr. B. Jaduszliwer for a critical reading of the manuscript. This work was supported by the Aerospace Sponsored Research Program.

[1] U. Cappeller and H. Mueller, Ann. Phys. (Leipzig) **42**, 250 (1985).
[2] R. P. Frueholz and J. C. Camparo, Phys. Rev. A **47**, 4404 (1993).
[3] See, for example, M. W. Hamilton, K. Arnett, S. J. Smith, D.S. Elliot, M. Dziemballa, and P. Zoller, Phys. Rev. A **36**, 178 (1987).
[4] A. A. Popov, A. M. Shalagin, V. M. Shalaev, and V. Z. Yakhnin, Zh. Eksp. Teor. Fiz. **80**, 2175 (1981) [Sov. Phys. JETP **53**, 1134 (1981)].
[5] G. Vemuri and D. M. Wood, Phys. Rev. A **50**, 747 (1994).
[6] P. Thomann and G. Busca, J. Phys. (Paris) Suppl. Colloq. **C8**, 189 (1981).
[7] A. De Marchi, G. D. Rovera, and A. Premoli, IEEE Trans. Ultrason. Ferroelectr. Freq. Contr. **UFFC-34**, 582 (1987).
[8] E. B. Alexandrov and V. A. Bonch-Bruevich, Opt. Eng. **31**, 711 (1992).
[9] G. D. Rovera, G. Santarelli, and A. Clarion, Rev. Sci. Instrum. **65**, 1502 (1994).
[10] L. Allen and J. H. Eberly, *Optical Resonance and Two-Level Atoms* (Wiley, New York, 1975).
[11] I. I. Rabi, N. F. Ramsey, and J. Schwinger, Rev. Mod. Phys. **26**, 167 (1954).

[12] F.C. Moon and G.-X. Li, Physica D **17**, 99 (1985).
[13] J. C. Camparo and P. Lambropoulos, Phys. Rev. A **47**, 480 (1993).
[14] P. Avan and C. Cohen-Tannoudji, J. Phys. B **10**, 155 (1977).
[15] See, for example, S. Seely, *Electron-Tube Circuits* (McGraw-Hill, New York, 1950), pp. 486–487.
[16] P. G. Drazin, *Nonlinear Systems* (Cambridge University Press, Cambridge, England, 1992), Chap. 5.